Bioorg. Med. Chem. Lett. 47 (2021) 128202

Contents lists available at ScienceDirect

Bioorganic & Medicinal Chemistry Letters

journal homepage: www.elsevier.com/locate/bmcl

Development of potent and selective Cathepsin C inhibitors free of aortic binding liability by application of a conformational restriction strategy

Abhisek Banerjee [a], Ranganadh Velagaleti [a], Sandip Patil [a], Mahesh Pawar [a], Pravin Yadav [a], Pradip Kadam [a], Mohammad Mohsin Qadri [a], Samitabh Chakraborti [b], Jagmohan S. Saini [c], Dayanidhi B. Behera [d], Keya Karanjai [a], Pravin S. Iyer [a,b,c,d], Laxmikant A. Gharat [a], Sanjib Das [a,*]

[a] Medicinal Chemistry Division, Glenmark Research Centre, A-607, TTC Industrial Area, MIDC Mahape, Navi Mumbai 400 709, India.
[b] Pharmacology Division, Glenmark Research Centre, A-607, TTC Industrial Area, MIDC Mahape, Navi Mumbai 400 709, India.
[c] Computational Chemistry, Glenmark Research Centre, A-607, TTC Industrial Area, MIDC Mahape, Navi Mumbai 400 709, India.
[d] Drug Metabolism and Pharmacokinetics, Glenmark Research Centre, A-607, TTC Industrial Area, MIDC Mahape, Navi Mumbai 400 709, India

ARTICLE INFO

Keyword:
Chronic Obstructive Pulmonary Disease (COPD)
α-Amino acid based scaffold
Amidoacetonitrile-based Cathepsin C inhibitors
Coronavirus SARS-CoV-2
Aortic binding
Catalytic cysteine residue (Cys234)

ABSTRACT

Cathepsin C plays a key role in the activation of several degradative enzymes linked to tissue destruction in chronic inflammatory and autoimmune diseases. Therefore, Cathepsin C inhibitors could potentially be effective therapeutics for the treatment of diseases such as chronic obstructive pulmonary disease (COPD) or acute respiratory distress syndrome (ARDS). In our efforts towards the development of a novel series of Cathepsin C inhibitors, we started working around AZD5248 (**1**), an α-amino acid based scaffold having potential liability of aortic binding. A novel series of amidoacetonitrile based Cathepsin C inhibitors were developed by the application of a conformational restriction strategy on **1**. In particular, this work led to the development of a potent and selective Cathepsin C inhibitor **3p**, free of aortic binding liability.

Cathepsin C (Cat C), also known as dipeptidyl peptidase I (DPP I), is a constitutively expressed lysosomal cysteine protease which sequentially removes dipeptides with broad specificity from the free *N*-terminal of proteins and peptides.[1] Many members of the Cathepsin family are important for intracellular protein degradation and cellular homeostasis. While Cathepsin C plays a crucial role in these processes, it also activates a number of granule-associated serine proteases with pro-inflammatory and immune functions. Some of the downstream proteases matured by Cathepsin C are neutrophil elastase (NE), cathepsin G (Cat G) and proteinase-3 (PR- 3), which are present in neutrophils as well as in macrophages. Additionally, mast cell proteases and granzymes, present in cytotoxic T lymphocytes (CTLs) and natural killer (NK) cells, are also matured by Cathepsin C.[2] Maturation of these downstream proteases result in degradation of extracellular matrix (ECM) components, cleavage of inflammatory mediators, cytokine as well as chemokine induction, increased chemotaxis, increased airway secretions and maintenance of inflammation.[3]

A number of respiratory diseases are associated with an over-abundant accumulation of neutrophils and the presence of increased levels of at least some neutrophil serine proteases. These enzymes are believed to play a role in the pathology of several respiratory diseases, such as Chronic Obstructive Pulmonary Disease (COPD), Cystic Fibrosis (CF), non-Cystic Fibrosis (non-CF), bronchiectasis and also ARDS associated with COVID-19 infections.[4]

Cat C knockout mice are resistant to lung airspace enlargement and inflammatory cell infiltration in both cigarette smoke and ozone exposure models of COPD.[5,6] The pharmacological inhibition of Cat C activity via therapeutic administration of the covalent, irreversible compound, MOTP, results in protection from smoke-induced pulmonary inflammation, and alveolar destruction comparable to the levels of protection exhibited by Cat $C^{-/-}$ mice. The results suggest Cat C as a potential target for new therapies addressing unmet needs in chronic respiratory diseases and emphysema.[7] Brensocatib (AZD7986, **2** in Fig. 1), a Cat C inhibitor from Astrazeneca/Insmed, has been reported to achieve its primary end-point in a Phase II clinical trial with non-cystic fibrosis bronchiectasis patients. Moreover, the company announced very recently that brensocatib will be evaluated in the STOP-COVID19 (Superiority Trial of Protease Inhibition in COVID-19, EudraCT no. 2020–001643-13) trial in up to 300 hospitalized patients with COVID-19. The eventualities in COVID-19 often result from acute respiratory

* Corresponding author.
E-mail address: Sanjib.Das@glenmarkpharma.com (S. Das).

https://doi.org/10.1016/j.bmcl.2021.128202
Received 25 February 2021; Received in revised form 5 June 2021; Accepted 10 June 2021
Available online 15 June 2021

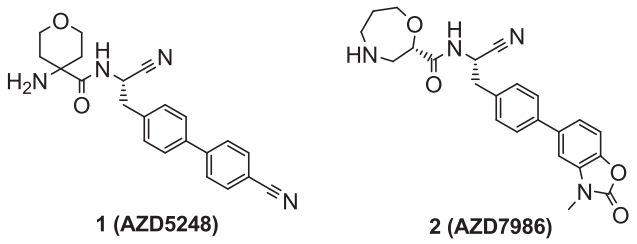

Fig. 1. Cat C inhibitors developed by AstraZeneca.

distress syndrome (ARDS). Accumulated evidence indicates that lung injury in such cases result due to release of proteases from activated neutrophils.[8] As seen previously in chronic respiratory syndromes, Cat C might be a major driver of lung damage and hence, inhibition of this upstream protease can fulfil an important medical need in this pandemic situation. Given such findings, Cat C has been recognized as a potential therapeutic target for the treatment of a broad range of diseases due to the important role that it plays in biological systems. Thus, an object of the present invention is to provide compounds which are inhibitors of Cathepsin C.

Many organizations like, GlaxoSmithKline, AstraZeneca, Boehringer Ingelheim, Prozymex and Janssen have been extensively working on Cat C as a therapeutic target over the years. Around thirty-five international patent publications disclose variety of scaffolds as Cat C inhibitors.[9,10] Many known Cat C inhibitors form an irreversible covalent bond with Cys-234 of the enzyme's active-site. Typically, these inhibitors are dipeptides carrying reactive functional groups such as diazomethyl ketones,[11,12] vinyl sulfones,[13,14] acyloxymethyl and fluoromethyl ketones,[13] and *O*-acyl hydroxamic acids.[15] In addition, naturally occurring epoxysuccinyl derivative E64 was also shown to inhibit Cat C at high concentrations.[16] Known reversible inhibitors of Cat C are dipeptide semicarbazides,[17] arginine-based peptides,[18] phosphinic tripeptides[19] and dipeptide nitriles.[20–23]

Most recently, AstraZeneca reported potent and selective dipeptide nitrile based Cat C inhibitors **1 (**AZD5248) and **2** (AZD7986) (Fig. 1). In particular, AstraZeneca's first generation Cat C inhibitor **1** showed aortic binding in a rat quantitative whole body autoradiography. As a result, its development was terminated before human dosing due to safety concerns. The chemical reactivity of α-amino acid structure of **1** with an aldehyde of elastin peptide chain (Scheme 1) from aortic tissue is responsible for the toxicity.[2,24]

Specifically, the chemical reactivity of 4-aminotetrahydro-2*H*-pyran-4-carboxamide of **1** with the aldehyde of elastin occurs through formation of a stable five-membered imidazolidin-4-one (Scheme 1). AstraZeneca overcame this aortic binding liability by employing *β*-amino acids and ultimately developed second generation Cat C inhibitor **2** (Fig. 1), which was in Phase II clinical trials for treatment of COPD.[24] In our hands, we could reproduce the reactivity profiles of **1** (fast; 15% remaining after 1 h) and **2** (slow; 95% remaining after 15 h) in propionaldehyde based *in vitro* chemical reactivity assay,[25] developed to support lead optimization process by eliminating the possibility of aortic binding. (Table 4).

In our quest, we envisioned that *α*-amino acids with appropriate conformational constrain around the reactive amino group on **1** (Fig. 1), can overcome this aortic binding liability. To test the hypothesis, a series of novel Cat C inhibitors with variety of α -amino acids, with different degrees of conformational constrain, were synthesized (**3a-q**) and screened (Tables 1–3). During this exercise, ([1,1′-biphenyl]-4-yl)propanenitrile portion of **1** (Fig. 1) was kept constant. Together with **1** and **2**, selected compounds were screened against propionaldehyde based *in vitro* assay (Table 4).

The preparations of compounds **3a-3q** were achieved using the general synthetic route illustrated in Scheme 2. As previously reported, amine **7**[2] was synthesized from compound **4** *via* sequential *N*-Boc protection, amidation, Suzuki coupling with (4-cyanophenyl)boronic acid and *N*-Boc deprotection. The obtained amine **7** was then coupled with various known and novel *N*-Boc-protected cyclic *α*-amino acids **8a-q**

Table 1

Cat C inhibitors with 6-membered *α*-amino acids.

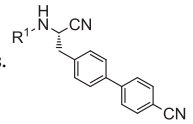

Compound	R^1	% Cat C Inhibition (1 μM)	% Cat C Inhibition (10 μM)	Cat C Enzyme IC_{50} (nM)[a]	Cat C Cellular IC_{50} (nM)[a]
1		99.2	99.9	1	5
3a	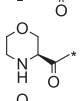	75.54	96.31	308.1	9724
3b		2.2	14.2	ND[b]	ND[b]
3c	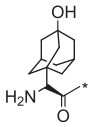	3.29	2.19	ND[b]	ND[b]
3d	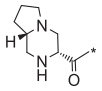	68.26	94.99	394	ND[b]
3e	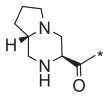	1.2	0	ND[b]	ND[b]
3f	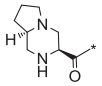	4.63	22.75	ND[b]	ND[b]
3g	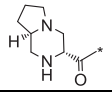	1.11	1.11	ND[b]	ND[b]

[a] Values are mean of two independent experiments in duplicate.
[b] ND refers to 'not determined'.

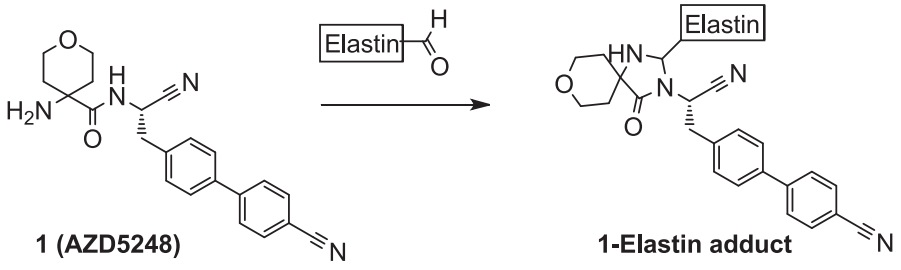

Scheme 1. Imidazolidin-4-one formation of **1** with elastin.

Table 2

Cat C inhibitors with 5-membered spiro α-amino acids.

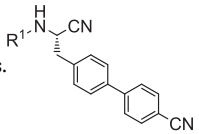

Compound	R^1	% Cat C Inhibition (1 μM)	% Cat C inhibition (10 μM)	Cat C Enzyme IC_{50} (nM)[a]	Cat C Cellular IC_{50} (nM)[a]
3h		91.47	99.07	91.51	ND[b]
3i		92.36	99.49	77.56	ND[b]
3j		97.19	98.19	27.83	150.3
3k		99.04	99.67	10.17	68.98
3l	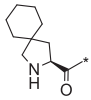	84.3	99.32	227.9	ND[b]

[a] Values are mean of two independent experiments in duplicate.
[b] ND refers to 'not determined'.

(Scheme 3 and 4) to provide amides **9a-q**. Subsequent dehydration provided nitriles **10a-q** which upon *N*-Boc deprotection provided compounds **3a-q**.

In particular, *N*-Boc amino acids **8a-8c** and **8h** were commercially available, whereas **8d-8g** were synthesized as previously reported.[26] Spiro *N*-Boc aminoacids **8i-8l** are also commercially available, however, they were synthesized using a modified synthetic strategy as illustrated in Scheme 3.[27] O-Benzylation of commercially available chiral alcohol **11**[28] followed by epoxide opening with cyclic carbonitriles **12i-l**, provided nitriles **13i-l**.[29–31] Subsequent nitrile reduction and *N*-Boc protection provided amino alcohols **14i-l** which upon intramolecular cyclization yielded benzyl ethers **15i-l**.[32] O-Debenzylation by hydrogenolysis provided corresponding amino alcohols **16i-l**, which upon oxidation provided *N*-Boc amino acids **8i-l**.

N-Boc amino acids **8m**,[33] **8o**,[34] **8p**,[35] and **8q**[36] are known and synthesized as previously reported. Novel *N*-Boc amino acid **8n** was synthesized as illustrated in Scheme 4.[37] Reductive amination of keto ester **17** with (*R*)-(+)-α-methylbenzylamine provide amino ester **18**[38] which upon further reduction provided amino alcohol **19**. Subsequent *N*-alkylation of **19** with ethyl bromoacetate provided amino alcohol **20**, which upon mesylation and intramolecular *c*-alkylation provided bicyclic amino ester **21**. *N*-Dealkylation and *in situ* Boc-protection was followed by ester hydrolysis to provide *N*-Boc amino acid **8n**.

A quick structure–activity relationship (SAR) of 6-membered α-amino acids (**3a** – **3g**, Table 1) was established around compound **1** (AZD5248), which showed potent human Cat C inhibition with enzyme IC_{50} of 1 nM and cellular IC_{50} of 5 nM. Compound **3a** showed moderate Cat C enzyme inhibition with IC_{50} 308.1 nM, whereas its diastereomer **3b** showed poor Cat C inhibition (2.2% and 14.2% inhibition at 1 μM and 10 μM concentration, respectively). 3-Hydroxyadamantanyl-α-amino acid derivative **3c** also appeared inactive in our assay. Except for **3d** (Cat C IC_{50} = 394 nM), remaining conformational restricted 6-membered α-amino acids (**3e-3g**, Table 1) showed poor Cat C inhibition at both 1 μM and 10 μM concentrations.

At this stage, we turned our attention to 5-membered ring α-amino acids (**3h** – **3l**, Table 2). Compound **3h** with a simple 5-membered α-amino acid (proline) showed Cat C enzyme inhibition with IC_{50} = 91.51 nM. However, as anticipated, it indicated fast aortic binding (8% remaining after 2 h; half-life of 0.56 h) when tested in the propionaldehyde reactivity assay (Table 4). To get rid of the aortic binding liability, spiro analogs of various ring sizes (3–6) by systematic homologation on proline were pursued (**3i-3l**). In comparison to **3h**, increase in Cat C enzymatic potency was observed from 3-membered ring to 5-membered ring (**3i**: IC_{50} = 77.56 nM; **3j**: IC_{50} = 27.83 nM; **3k**: IC_{50} = 10.17 nM), whereas, 6-membered ring (**3l**) was less potent (IC_{50} = 227.9 nM). In addition, increase in cellular potency was also observed from **3j** (IC_{50} = 150.3 nM) to **3k** (IC_{50} = 68.98 nM) with increase in ring size. At this stage, the most potent compound from this series **3k** was advanced for aldehyde binding studies; however, this analog too showed tendency of fast aortic binding (0% remaining after 15 h; half-life of 0.56 h; Table 4).

Table 3

Cat C inhibitors with fused 5-membered α-amino acids.

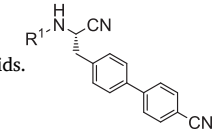

Compound	R^1	% Cat C inhibition (1 μM)	% Cat C inhibition (10 μM)	Cat C Enzyme IC_{50} (nM)[a]	Cat C CellularIC_{50} (nM)[a]
3m		83.89	97.87	222.6	ND[b]
3n		6.55	50.15	ND[b]	ND[b]
3o		85.61	98.23	77.73	79.07
3p		99.18	99.96	9.27	699.2
3q	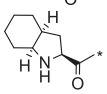	88.72	99.03	153.6	1716

[a] Values are mean of two independent experiments in duplicate.
[b] ND refers to 'not determined'.

Table 4
Cathepsin aldehyde adduct assay.

Compound	MW	Propionaldehyde Reaction[a]	MW of Adduct[b]	% Remaining[c]	Duration of Incubation (h)	Half-life of Analyte (h)
1	374.4	Fast	414	15	1	0.36
2	420.5	Slow	NT[d]	95	15	> 15
3a	360.41	Moderate	399 (NEG)	48	15	15.75
3h	344.4	Fast	383 (NEG)	8.5	2	0.56
3k	398.5	Fast	437 (NEG)	0	15	0.56[e]
3n	384.5	Slow	423 (NEG)	100	15	–
3o	384.5	Fast	423 (NEG)	7	15	5.3
3p	384.5	Slow	NT[d]	97	15	> 15

[a] Stability was evaluated for all the compounds in a single experiment using bulk spiking (n = 1), wherein the compound was spiked into the solution of propionaldehyde in 0.1 M phosphate buffer (pH 7.4); samples were aliquoted at intervals and analyzed in HPLC-UV.
[b] Mass of the adduct was confirmed as addition of (+) 40 amu to respective molecular ion peak.
[c] In-house data based on hour of incubation with propionaldehyde.
[d] NT- Not tested as compound was not reactive.
[e] Only 2 h data considered for calculation of $t_{1/2}$ as no area of analyte observed in 15 h.

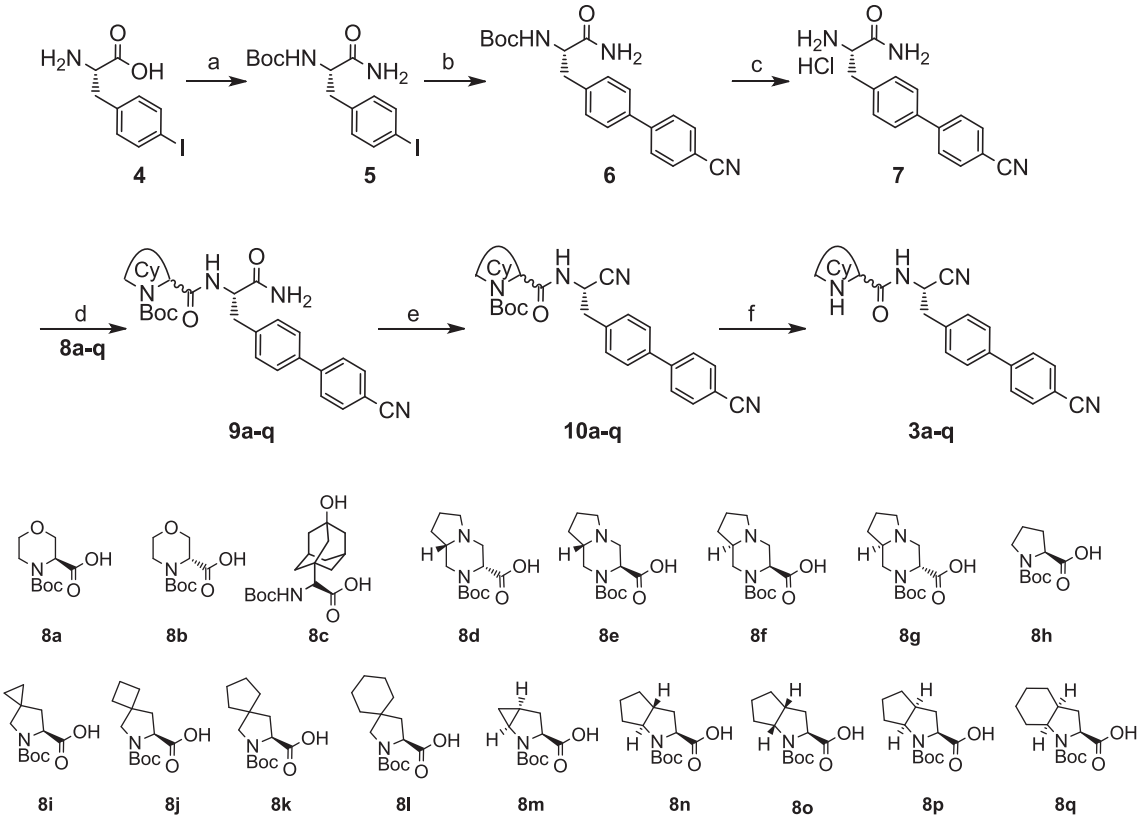

Scheme 2. Reagents and conditions: (a) (i) di-*tert*-butyl dicarbonate, Na_2CO_3, H_2O, THF, RT, 48 h, 80% (ii) NH_4Cl, HATU, HOBt, DIPEA, DMF, RT, 16 h, 96%; (b) (4-cyanophenyl)boronic acid, Pd(dppf)Cl_2.CH_2Cl_2, K_2CO_3, 1,4-dioxane, H_2O, 80 °C, 18 h, 50%; (c) HCl in diisopropyl ether, THF, 10 °C, 4 h, 96%; (d) (i) Acid **8a-q**, HATU, HOBt, DIPEA, DMF, RT, 18 h, 50–60%; (e) Burgess reagent, CH_2Cl_2, RT, 18 h, 80–90%; (f) Formic acid, THF, 0 °C - RT, 18 h, 20–30%.

Then, we shifted our focus to fused bicyclic ring system where *α*-amino acid proline was kept constant (**3m-3q**, Table 3). Compound **3m** (IC_{50} = 222.6 nM) with a 3-membered fused ring was equipotent to **3l**, but was much less active compared to **3h-3k** (Table 2). This difference in potency opened up a possibility of occupying the available space with right orientation so that the enzymatic potency can be improved. 5-membered fused ring with a *trans*- ring junction (**3n**) and two possible *cis*- ring junctions (**3o** and **3p**) were prepared. To our delight, the enzymatic potency improved significantly from **3n** (50% inhibition at 10 μM, Table 3) to **3p** (IC_{50} = 9.27 nM). However, with the introduction of 6-membered fused ring (**3q**), there was a 16-fold drop in potency (IC_{50} = 153.6 nM).

The difference in potency between compounds **3n**, **3o** and **3p** were in accordance to our docking experiments performed using Schrodinger's Glide module.[39] The X-ray crystal structure of Cat C (PDB Code: 4CDE) is used to perform all docking studies (Figure 2).[2] Structural information revealed human Cat C to exist in a tetrameric form containing four identical subunits.[1] Each identical subunit comprises of three chains, light and heavy chains forming the catalytic domain, and a third chain constituting the exclusion domain. The active site of the protein harbors the catalytic cysteine residue (Cys234), which is located at the interface of these three chains. Cat C has an open S1 pocket located at the entrance of the active site, and a large S2 pocket which is deeply buried within the protein. The exclusion domain, a unique characteristic of Cat C, blocks access of substrates beyond the S2 site and explains the exopeptidase activity of Cat C. In addition, the side chain of Asp1 located in the

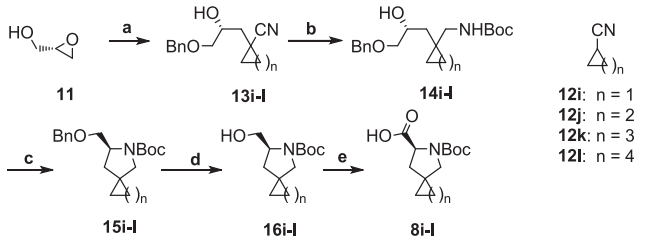

Scheme 3. Reagents and conditions: (a) (i) Benzyl bromide, NaH, THF, RT, 5 h, 56% (ii) cyclic carbonitrile **12i-l**, diisopropylamine, *n*-BuLi, THF, −78 °C, 1 h, 40–55%; (b) cobalt (II) chloride hexahydrate, $NaBH_4$, MeOH, RT, 1 h, di-*tert*-butyl dicarbonate, NaOH, H_2O, CH_2Cl_2, RT, 18 h, 80–85%; (c) trimethyl orthoacetate, BF_3 etherate, CH_2Cl_2, RT, 2 h 40–50%; (d) H_2, 10% Pd on carbon (wet), MeOH, 40 psi, RT, 2 h, RT, 90–95%; (e) 4-methylmorpholine *N*-oxide, tetrapropylammonium perruthenate, CH_3CN, RT, 2 h, 95–98%

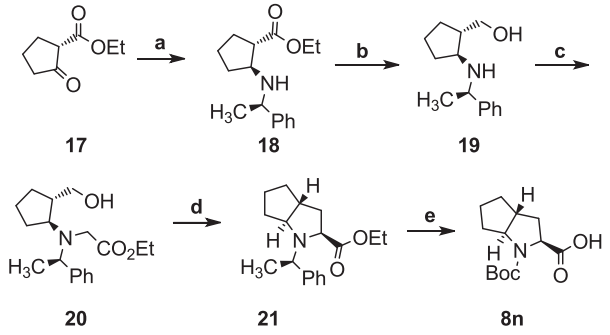

Scheme 4. Reagents and conditions: (a) (*R*)-(+)-α-methylbenzylamine, AcOH, ethanol, 70–75 °C, 4 h, then sodium cyanoborohydride, reflux, 12 h, 24%; (b) lithium triethylborohydride solution (1 *M* in THF), RT, 3 h, 80%; (c) ethyl bromoacetate, $NaHCO_3$, CH_3CN, reflux, 14 h, 72%; (d) (i) methanesulfonyl chloride, triethylamine, CH_2Cl_2, 0 °C -RT, 30 min, 93% (ii) sodium *tert*-butoxide, THF, 70–80 °C, 5 h, 33%; (e) (i) di-*tert*-butyl dicarbonate, palladium on carbon (10% wet), EtOH, H_2, 60 psi, RT, 18 h, 81% (ii) lithium hydroxide, THF, methanol, RT, 18 h, 87%.

exclusion domain governs substrate recognition by interacting with the α-amino group of the substrate peptide.[24] Critical residues that form the hot-spots for ligand–protein interactions are Cys234 (responsible for covalent bond formation), Gly277, Asn380, Asn 65 and Asp1. From the docked-ligand pose analysis, it is observed that all three compounds **3p**, **3o** and **3n** make covalent interaction with Cys234 and hydrogen bond interaction with Gln228. Furthermore, it was seen that cyano (CN) group in compound **3p** makes a stable hydrogen bond with Asn65, which is missing in compound **3o**.[40] Lack of this interaction could be attributed to the reduced potency of **3o**. The (2*S*)-octahydrocyclopenta [*b*]pyrrole-ring forms a hydrogen bond with residues Gly277 and Asp1 in both compounds **3p** and **3o**, whereas in compound **3n,** interaction with Asp1 is missing due to change in chiral center and rotation of the bicyclic ring. The absence of this critical interaction might be responsible for loss in potency of compound **3n**.

Compound **3p** proved to be the first Cat C inhibitor from this series with significantly reduced aortic binding tendency (97% remaining after 15 h; half-life > 15 h) in propionaldehyde studies (Table 4). In contrast, its diastereomer **3o** had higher aortic binding possibility (7% remaining after 15 h; half-life = 5.3 h). In addition, the less active analog **3n** also showed reduced aortic binding (100% remaining after 15 h) tendency. Overall, compound **3p** not only well occupied the S2 pocket with its fused ring system to provide high potency, but also the conformational rigidity of the ring junction kept the two nitrogen far enough such that the imidazolin-4-one formation with aldehyde was not feasible.

Table 5

SAR and metabolic stability data of **24a-e.**

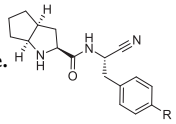

Compound	R	Cat C IC_{50} (nM)[a]	Metabolic stability (% remaining)[b]		
			Human	Rat	Mouse
3p		9.27	1 ± 0.5	3 ± 0.6	6 ± 0.5
24a	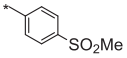	44.01	14 ± 1.0	25 ± 2.7	32 ± 3.4
24b		4.62	16 ± 0.5	0 ± 0.0	12 ± 2.0
24c		14.89	2 ± 0.2	2 ± 0.9	16 ± 6.0
24d	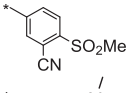	6.45	9 ± 0.3	34 ± 5.2	47 ± 5.4
24e	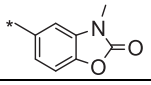	1248	8 ± 0.7	29 ± 3.9	22 ± 1.5

[a] values are reported as mean of three replicates (±SD).
[b] Percentage remaining at 60 min in liver microsomal preparations.

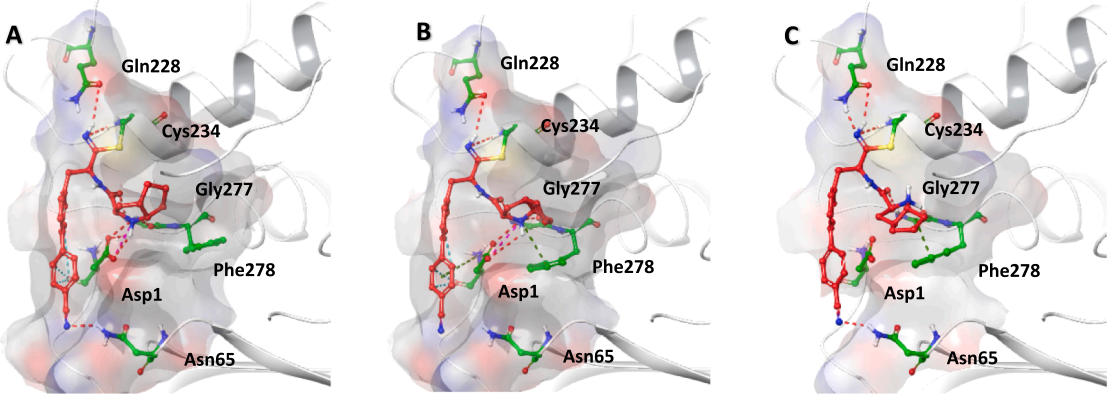

Fig. 2. Docking of Compounds **3p** (A), **3o** (B) and **3n** (C) in the binding pocket of Cat C (PDB 4CDE). Indicated in the figures are the key hydrogen bonds between the protein and ligands within a distance of 4 Å. (A) **3p** makes interactions with Asp1, Cys234, Gln228, Gly277 and Asn65 (B) **3o** makes interactions with Asp1, Cys234, Gln228, Gly277; Asn65 interaction is missing (decreased potency) (C) **3n** does not make critical interactions with Asp1 due to rotation of the bi-cycle; Asp1 is critical residue reported for activity.

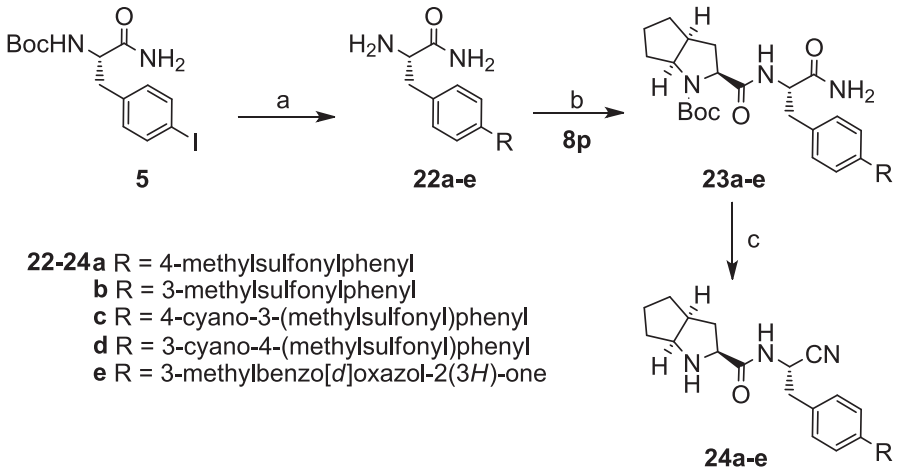

Scheme 5. Reagents and conditions: (a) (i) substituted boronic acid, $Pd(dppf)Cl_2.CH_2Cl_2$, K_2CO_3, 1,4-dioxane, H_2O, 80 °C, 18 h, 50–55% (ii) HCl in diisopropyl ether, THF, 10 °C, 4 h, 95–98%; (b) (i) Acid **8p**, HATU, HOBt, DIPEA, DMF, RT, 18 h, 50–60%; (c) (i) Burgess reagent, CH_2Cl_2, RT, 18 h, 80–90% (ii) Formic acid, THF, 0 °C - RT, 18 h, 25–30%.

Table 6
Selectivity profile for **3p.**

Enzyme	Fold selectivity	% inhibition (1 μM)	% inhibition (10 μM)
Cathepsin K	93		
Cathepsin L	10,780		
Cathepsin S	4405		
Cathepsin B	2260		
CYP1A2		15.2	43.7
CYP2D6		69.7	88.3
CYP3A4		2.2	33.8
CYP2C9		12	32.4
CYP2C19		17.1	38.4
CYP2C8		11.8	40.1

Therefore, the difference in reactivity towards aldehyde binding assay with various diastereomers clearly supported our hypothesis that α-amino acids with appropriate conformational rigidity on **1** (Figure 1) can overcome this aortic binding liability.

With encouraging data of compound **3p** from aldehyde binding assay, we developed a quick SAR around the 4-cyano group (Table 5). The compounds **24a-e** were synthesized by following the strategy illustrated in Scheme 5, starting with 4-iodophenyl derivative **5**. The synthetic route followed was the same as described in scheme 2 for the preparation of compounds **3a-q**.

The replacement of 4-cyano group of **3p** with 4-methylsulfone **24a** resulted in a 5-fold drop in potency and marginal improvement in metabolic stability across all the species. On the other hand, analogs **24b-d** were at par with **3p** in terms of potency and metabolic stability. 3-Methylbenzooxazolone substitution in case of **24e**, caused>100-fold drop in potency to 1.2 μM. Overall, compounds **24a-e** showed very poor metabolic stability against human microsome and low to moderate stability against rodent microsomes.

3p was found to be selective for Cathepsin C over Cathepsins K, L, S and B. In addition, it did not show significant inhibition of CYP450 enzymes except CYP2D6 (Table 6). However, this compound was rapidly metabolized in human, mouse and rat liver microsomes but stable in plasma as tested *in vitro* (data not shown).

In conclusion, we have identified **3p**, a potent and selective α-amino acid based Cat- C inhibitor devoid of aortic binding possibilities. In addition, it showed weak inhibition of the CYP450 enzymes except CYP2D6 and having reasonably good selectivity over Cathepsins K, L, S and B. Poor metabolic stability of **3p** encouraged us to explore the opportunity of developing it for inhaled therapy to minimize the systemic side effects of Cathepsin C inhibitors. Further efforts towards the development of **3p** or a close analog, as an inhaled therapeutic agent will be reported in due course.

Declaration of Competing Interest

The authors declare that they have no known competing financial interests or personal relationships that could have appeared to influence the work reported in this paper.

Acknowledgements

We thank the analytical team (NCE Research) for all the analytical support related to this publication. We also thank Glenmark Pharmaceuticals Limited for providing research facilities and consent for publication.

Appendix A. Supplementary data

Supplementary data to this article can be found online at https://doi.org/10.1016/j.bmcl.2021.128202.

References

1 Turk D, Janjić V, Stern I, et al. *EMBO J*. 2001;20:6570.
2 Furber M, Tiden A, Gardiner P, et al. *J Med Chem*. 2014;57:2357.
3 Korkmaz B, Horwitz MS, Jenne DE, Gauthier F. *Pharmacol Rev*. 2010;62:726.
4 Korkmaz B, Caughey GH, Chapple I, et al. *Pharmacol Ther*. 2018;190:202.
5 Guay D, Beaulieu C, Percival MD. *Curr Top Med Chem*. 2010;10:708.
6 Podolin PL, et al. *Inflammation Research*. 2008;57(Suppl 2):S104 (Symposium Abstract).
7 Podolin PL, Bolognese BJ, Foley JP, et al. *Am J Respir Crit Care Med*. 2013;187: A1500. www.atsjournals.org (Symposium Abstract funded by GlaxoSmithKline).
8 Korkmaz B, Lesner A, Marchand-Adam S, Moss C, Jenne DE. *J Med Chem*. 2020;63: 13258.
9 Laine DI, Busch-Petersen J. *Expert Opin Ther Pat*. 2010;20:497.
10 Selected International Patent Publications viz., WO 2010128324, WO 2010142985, WO 2011025799, WO 2011075631, WO 2011154677, WO 2012119941, WO 2012109415, WO 2012112733, WO 2013041497, WO 2014140081, WO 2014140078, WO 2014140091, WO 2014140075, WO 2014091443, WO 2015032942, WO 2015110826, WO 2016016242, WO 2016038007 and WO 2020001392.
11 Thiele DL, Lipsky PE, McGuire MJ. *U.S. Patent*. 1997;5602:102.
12 Green GDJ, Shaw E. *J Biol Chem*. 1923;1981:256.
13 Kam C-M, Götz MG, Koot G, et al. *Arch Biochem Biophys*. 2004;427:123.
14 Yuan F, Verhelst SHL, Blum G, Coussens LM, Bogyo M. *J Am Chem Soc*. 2006;128: 5616.
15 Demuth H-U, Heiser U, Niestroj A. *WO*. 2003;03022871:A2.
16 Barrett AJ, Kembhavi AA, Brown MA, et al. *Biochem J*. 1982;201:189.
17 Bondebjerg J, Fuglsang H, Valeur KR, et al. *Bioorg Med Chem*. 2005;13:4408.
18 Horn M, Pavlik M, Doleckova L, Baudys M, Mares M. *Eur J Biochem*. 2000;267:3330.
19 Mucha A, Pawelczak M, Hurek J, Kafarski P. *Bioorg Med Chem Lett*. 2004;14:3113.

20 Thompson SA, Andrews PR, Hanzlik RP. *J Med Chem.* 1986;29:104.
21 Bondebjerg, J.; Fuglsang, H.; Naerum, L. WO2004110988, 2004.
22 Bondebjerg J, Fuglsang H, Valeur KR, Pedersen J, Naerum L. *Bioorg Med Chem Lett.* 2006;16:3614.
23 Guay D, Beaulieu C, Truchon JF, et al. M. *Bioorg Med Chem Lett.* 2009;19:5392.
24 Doyle K, Lonn H, Kack H, et al. *J Med Chem.* 2016;59:9457.
25 Bragg RA, Brocklehurst S, Gustafsson F, et al. *Chem Res Toxicol.* 1991;2015:28.
26 Falorni M, Porcheddu A. *Giacomelli G. Tetrahedron: Asymm.* 1999;1996:7.
27 Bryans JS, Horwell DC, Receveur, J-M. WO1999061424A1, 1999.
28 Taylor CA, Zhang Y-A, Snyder S. A. *Chem Sci.* 2020;11:3036–3041.
29 Taber DF, Kanai K, Jiang Q, Bui G. *J Am Chem Soc.* 2000;122:6807–6808.
30 Xu F, Murry JA, Simmons B, et al. *Org Lett.* 2006;8:3885–3888.
31 Takahashi M, Shioura Y, Murakami T, Ogasawara K. *Tetrahedron-Asymmetry.* 1997;8:1235–1242.
32 Park H, Kwon Y, Shin JE, et al. *Synthesis.* 2017;49:2761–2767.
33 Lopez, O. D.; St. Laurent, D. R.; Goodrich, J.; Romine, J. L.; Serrano-Wu, M.; Yang, F.; Kakarla, R.; Yang, X.; Qiu, Y.; Snyder, L. B. US 20110294819, 2011.
34 Harwood LM, Lilley IA. *Tetrahedron Lett.* 1993;34:537.
35 Kretzschmar, G.; Oehme, J.; Rossen, K. WO 2015189108, 2015.
36 Wang S, Su M, Wang J, et al. *Bioorg Med Chem.* 2014;22:6684.
37 Chemburkar, S. R.; Reddy, R. E.; Reamer, D. M.; Pavlina, J. T. Ulrey, S. S.; Kotecki, B. J. WO 2011009021, 2011.
38 LePlae PR, Umezawa N, Lee H-S, Gellman S. H. *J Org Chem.* 2001;66:5629–5632.
39 Halgren TA, Murphy RB, Friesner RA, et al. *J Med Chem.* 2004;47:1750.
40 Wang Y, Du Y, Huang N. *Future Med Chem.* 2018;10:2713–2728.